Release of functional dexamethasone by intracellular enzymes: A modular peptide-based strategy for ocular drug delivery

Madhushree Bhattacharya[a,b,*], Amir Sadeghi[b], Sanjay Sarkhel[a], Marja Hagström[a], Sina Bahrpeyma[a,b], Elisa Toropainen[b], Seppo Auriola[b], Arto Urtti[a,b,c]

[a] *Drug Research Programme, Division of Pharmaceutical Biosciences, University of Helsinki, Helsinki, Finland*
[b] *School of Pharmacy, University of Eastern Finland, Kuopio, Finland*
[c] *Institute of Chemistry, Saint-Petersburg State University, Peterhoff, Russian Federation*

ARTICLE INFO

ABSTRACT

Tissue barriers limit drug delivery in the eye. Therefore, retinal diseases are treated with intravitreal injections. Delivery systems with reduced dosing frequency and/or cellular drug delivery properties are needed. We present here a modular peptide-based delivery system for cell targeted release of dexamethasone in the retinal pigment epithelial cells. The peptide–dexamethasone conjugates consist of cell penetrating peptide, enzyme cleavable linker and dexamethasone that is conjugated with hydrazone bond. The conjugates are chemically stable in the vitreous, internalize into the retinal pigment epithelial cells and release dexamethasone intracellularly by enzymatic action of cathepsin D. *In vitro* binding assay and molecular docking confirm binding of the released dexamethasone fragment to the human glucocorticoid receptor. *In vivo* rabbit studies show increased vitreal retention of dexamethasone with a peptide conjugate. Modular peptide conjugates are a promising approach for drug delivery into the retinal cells.

1. Introduction

Ocular drug delivery poses significant challenges due to the unique anatomy and physiology of the eye. Various static and dynamic barriers limit efficient drug delivery, particularly to the posterior segment of the eye [1–3]. Therapeutic intervention of the posterior segment is crucial for many vision-threatening diseases, such as age-related macular degeneration, glaucoma, macular edema, diabetic retinopathy, and uveitis. These diseases cause disorders in the retina and choroid, thereby leading to impaired vision and blindness in millions of patients worldwide.

Topical eye drops are useful in the treatment of anterior segment diseases in the eye but they are ineffective in the treatment of retinal diseases. Several tissue barriers and flow factors limit drug distribution from topical application site to posterior segment tissues [4–6]. Tight tissue barriers between blood stream and ocular compartments (anterior, posterior) prevent drug distribution from the blood circulation into the ocular drug target tissues [7]. Alternative modes of ocular drug administration, such as sub-conjunctival, suprachoroidal, and periocular injections, have only achieved sub-optimal retinal drug delivery [8]. For these reasons, intravitreal injections are widely used even though it is an invasive method of retinal drug delivery. In the case of intravitreal drug delivery, it is important to ascertain delivery to the retinal target cells and adequate duration of drug action. Consequently, novel drug delivery systems are needed for intravitreal drug administration [9].

Current drug delivery systems for clinical treatment of the posterior segment diseases include intravitreal injection of drug solutions and implants [10,11]. For example, Ozurdex is a dexamethasone releasing injectable, degradable implant that is used to treat macular edema and inflammation of the eye [12]. Nonetheless, many implants comprise of non-degradable polymers that are used to control drug release for several months and might require surgical intervention; limiting their wide-spread clinical use [13,14]. Also, particulate based systems for intravitreal administration have been investigated [6]. Both implants and particulate systems might however obstruct vision and possible toxicity arising from polymer degradation products is of concern. Furthermore, their physical size does not allow targeted delivery to the retinal cells [5]. Development of alternative drug delivery systems are thus needed to meet the therapeutic challenges of retinal diseases.

Intravitreally administered small molecules are rapidly eliminated from the vitreous and they distribute non-specifically to ocular tissues and may cause adverse effects, such as increased intraocular pressure and cataract associated with corticosteroid treatment [4,15]. One

approach to mitigate side effects and rapid elimination of small molecule drugs is to form drug conjugates for targeted delivery and controlled release. Polymeric and antibody drug conjugates have been well investigated in the context of cancer therapy [16], but this concept has not been extensively explored for ocular drug delivery. A recent report introduced hyaluronic acid binding polypeptide chain to successfully prolong the half-life of protein drug [17]. We reported a peptide-based delivery system for controlled release of peptide cargo (D-peptides) within the intra-cellular space of the retinal pigment epithelial cells [18]. The peptide-based strategy utilized linkers that were cleaved by the enzymes present in the RPE cells to release the cargo. Additionally, the peptide-cargo conjugates were stable within the vitreous environment to avoid premature drug release in the vitreous. The modular delivery system consisted of three components: (a) cell penetrating peptide to promote intracellular entry, (b) peptide linker with controlled enzymatic cleavage rate and (c) D-peptide cargo. Notably, the peptide-based delivery system offers advantages of relative ease of synthesis, targeted intracellular delivery and controlled release of cargo exploiting intracellular components (enzyme cathepsin D) of the retinal cells.

In the present study, we demonstrate the potential of the modular peptide-based system for the retinal cellular delivery of dexamethasone. Dexamethasone is used in ophthalmology to treat ocular inflammations and uveitis in both anterior and posterior segments [19], but the use of dexamethasone is associated with side-effects, such as increased intraocular pressure and cataract formation [20]. Consequently, to overcome such effects, alternative delivery systems are desired for controlled or sustained release of dexamethasone at the site of action. We report here targeted and controlled release of dexamethasone from modular peptide-based delivery system within the retinal pigment epithelial cells.

2. Materials and methods

2.1. Design and synthesis of conjugates

2.1.1. Design of peptide-dexamethasone conjugates

A set of three peptide-dexamethasone conjugates (Scheme 1) were synthesized based on our previous findings [18]. The conjugates consisted of three components: (1) N-terminal cell penetrating peptide (CPP) to promote intracellular entry, (2) an enzyme cleavable peptide-based linker (PCL) and (c) dexamethasone conjugated to the C-terminal of PCL via hydrazone linkage. Fluorescent Alexa 488 dye was covalently attached to the conjugates. The differences between the three conjugates are entirely attributed to the CPPs with varying number of positively charged residues (Arg/Lys) (Scheme 1). Dex-1 contains a cationic CPP (from HIV-1 Tat) with 7 Arg/Lys residues, Dex-2 contains 2 Lys/Arg residues in the CPP sequence and Dex-3 consists of a

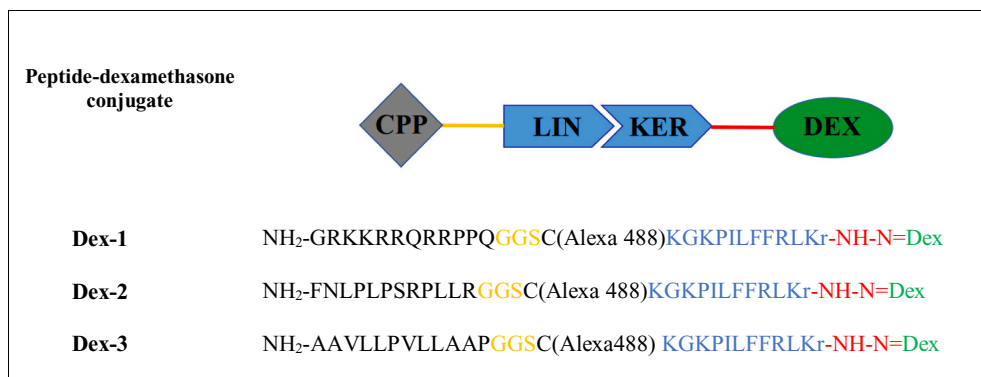hydrophobic CPP sequence [21].

2.1.2. Peptide synthesis

The peptide-dexamethasone conjugates (Scheme 1, Table 1) were synthesized by Peptide Synthetics Peptide Protein Research Ltd. (Hampshire, UK). In general, the peptides were synthesized using solid phase peptide synthesis. Chlorotrityl resin (Iris, 300 mg, per sequence, 200 mesh, 1.1 mmol/g chloride loading) was functionalized by mixing the resin in dry dimethyl formamide (DMF) with hydrazine (0.5 equivalents) for 30 min. Un-functionalized sites on the resin were capped with a brief treatment of methanol in DMF containing DIPEA (0.25 ml), to obtain a working substitution level of 0.3–0.5 mmol/g. The hydrazine resin obtained was then employed to generate peptides with the desired sequence via an automated peptide synthesizer (Symphony, Protein Technologies Inc. Arizona) using the Fmoc chemistry method [22] with Fmoc amino acids appropriately side chain protected (Matrix Innovation). After the synthesis, the hydrazide peptides were cleaved from the solid support and their side chain protecting groups were removed with trifluoroacetic acid (TFA) cocktail containing 2% isopropyl silane, 1% phenol and 2% ethane dithiol for 2 h. The TFA solution was filtered from the resin and the crude peptides precipitated by adding diethyl ether. The precipitated peptides were pelleted by centrifugation.

The peptides were purified by RP-HPLC on a Varian system equipped with a C-18 preparative Axia column (Phenomenex) at room temperature, using a Varian 325 UV-detector with a detection wavelength 225 nm, two 210 Varian pumps with flow rate of 20 ml/min and a gradient of 5–55% acetonitrile in 60 min. Peptides were loaded in dimethyl sulfoxide (DMSO) to the column and eluted with increasing gradient between water (with 0.1% TFA) and acetonitrile (with 0.1% TFA). The eluting peptides were visualized with UV absorption and the fractions were collected manually. The purity of the product-containing fractions was confirmed by LC-MS, combined and freeze-dried.

For peptide labeling with Alexa 488 dye, a cysteine residue was incorporated in the linker sequence between the CPP and PCL (Scheme-1). The side chain thiol of the cysteine was used to react with a maleimido-activated form of the Alexa 488 dye (Invitrogen): 5 mg of maleimido dye was added to the peptide (5 mg dissolved in 50:50 DMSO/PBS, pH 7.4, 2 ml). The mixture was stirred until all the peptide has been labeled (checked by mass spectrometry). Then, the peptide was introduced onto an HPLC column and the labeled peptide was eluted as described above. Purified labeled peptide was freeze-dried.

2.1.3. Synthesis of peptide-dexamethasone conjugates

The synthesized Alexa-labeled C-terminal peptide hydrazide was purified and then condensed with the ketone group of dexamethasone to form the hydrazone linked peptide-drug conjugate. In brief, the labeled peptide (2 mg) was dissolved in DMSO (0.5 ml) and sodium

Peptide-dexamethasone conjugate

Dex-1	NH₂-GRKKRRQRRPPQGGSC(Alexa 488)KGKPILFFRLKr-NH-N=Dex
Dex-2	NH₂-FNLPLPSRPLLRGGSC(Alexa 488)KGKPILFFRLKr-NH-N=Dex
Dex-3	NH₂-AAVLLPVLLAAPGGSC(Alexa488) KGKPILFFRLKr-NH-N=Dex

Scheme 1. Dexamethasone conjugated to the C-terminus of CPP-PCL chimeras via a hydrazone linkage (red). CPP, PCL sequences and dexamethasone are shown in black, blue and green, respectively. A short flexible linker, Gly-Gly-Ser (shown in yellow) was introduced in between the CPP and PCL sequences. A cysteine residue was introduced after the linker to attach the fluorescent dye Alexa 488 to the side chain thiol of Cys. Lower case single letter amino acid abbreviation refers to a D-amino acid. The D-amino acid enhances the sensitivity and specificity of the linker for cathepsin D mediated cleavage. (For interpretation of the references to color in this figure legend, the reader is referred to the web version of this article.)

Table 1
Peptide-dexamethasone conjugates and corresponding fragments after intracellular cleavage.

Conjugate #	Structure of the conjugates	Released fragment	Fragment mass	
			Calculated	Detected (MH^{+1} Mono)
Dex-1	NH$_2$-GRKKRRQRRPPQGGSC(Alexa 488)KGKPILFFRLKr-NH-N=Dex	r-NH-N=Dex	562.6	563.6
Dex-2	NH$_2$-FNLPLPSRPLLRGGSC(Alexa 488)KGKPILFFRLKr-NH-N=Dex	r-NH-N=Dex	562.6	563.6
Dex-3	NH$_2$-AAVLLPVLLAAPGGSC(Alexa488)KGKPILFFRLKr-NH-N=Dex	r-NH-N=Dex	562.6	563.6

Fragments were detected by LC-MS. r denotes D-Arginine residue.

acetate buffer (0.1 M, 0.5 ml) was added. A 10-fold molar excess of dexamethasone, pre-dissolved in DMSO, was added and the solution was stirred at 40 °C for 48 h. A further 10-fold molar excess of dexamethasone was added and mixed for another 48 h in case the reaction was not complete (as followed by LC/MS, Phenomenex C18 kinetex core-shell column, 50 × 4.6 mm, 2.6 μm internal diameter with a 100 Å pore size, step gradient of acetonitrile). When the reaction was completed (confirmed by LC/MS), the product was isolated by RP-HPLC as mentioned above.

2.2. In vitro stability and binding studies

2.2.1. Stability of conjugates in porcine vitreous

Stability of the peptide-dexamethasone conjugates against degradation in porcine vitreous was determined. Porcine eyes were procured from a local slaughterhouse and the eyes were kept on ice bath during the isolation of vitreous humor. The eyes were first cleansed of extra-ocular material and dipped in 70% ethanol. The eyes were opened by incision with a dissecting knife and the clear vitreous humor was separated gently from the retina. Isolated vitreous humor was homogenized, centrifuged (3200 ×g) for 1 h at +4 °C and the supernatant was sterile-filtered using a 0.22 μm filter to remove cellular debris and possible microbial contamination. The vitreous was stored at −80 °C. For stability studies, 10 μM of the conjugates were mixed with porcine vitreous humor with 1% antibiotics (penicillin/streptomycin; Gibco) in Eppendorff tubes. Each time point had designated separate tube. The tubes were incubated at 37 °C and release of dexamethasone from the conjugate was monitored using ultra-performance liquid chromatography tandem mass spectrometry (UPLC-MS/MS). Before the mass analysis, the mixture was subjected to acetonitrile clean-up. Three volumes of cold acetonitrile were added to each sample, vortexed and stored at room temperature for 1 h. The samples were centrifuged for 10 min at 12,000 ×g to remove precipitates. The supernatant was freeze-dried and stored at −20 °C for further UPLC-MS/MS analysis.

Liquid chromatography separation was carried out using Waters Acquity UPLC instrument (Waters, MA, USA) coupled with Waters Acquity UPLC BEH Shield RP18 (2.1 × 100 mm, 1.7 μm) column at 50 °C. The mobile phase consisted of 0.1% of formic acid in ultrapure water (A) and 100% of LC-MS grade acetonitrile (B). Freeze dried samples were diluted with cold 30% LC/MS grade acetonitrile (Chromasolv™, Honeywell, Seelze, Germany) in ultrapure water, and vortexed prior to the analysis. Mass spectrometry measurements were carried out using a Waters Xevo triple quadrupole mass spectrometer (TQ-S) equipped with an electrospray (ESI) source. Samples were analyzed on positive ionization mode and multiple reaction monitoring (MRM) mode was used for quantification. Minimum of five calibration curve points in the range 0.005–250 nM were used for quantification of the dexamethasone. The resulting data were analyzed with Waters MassLynx software V4.1.

2.2.2. Interactions of conjugates with the vitreous humor

Binding of peptide-dexamethasone conjugates to the porcine vitreous was studied by microscale thermophoresis (MST). MST is a biophysical technique used to study the molecular interaction by monitoring the directed movement of fluorescently labeled molecule in a temperature gradient [23–25]. The MST measurements were performed using a Monolith NT.115 instrument from Nanotemper Technologies (München, Germany) with MST grade premium NT.115 capillaries. Literature precedence's suggest that cationic particulate systems interact with hyaluronic acid, HA (anionic hydrophilic polymer), a primary component of the vitreous [26,27]. Consequently, for the positively charged peptide-dexamethasone conjugates, we postulate that they interact with vitreous HA. The concentration of HA in porcine vitreous (stock solution) was considered to be 1600 nM based on estimates from earlier reports [28,29]. The unlabeled vitreous (Section 2.2.1) was serially diluted and mixed with 100 nM fluorescently labeled conjugates in MST optimized buffer (50 mM Tris-HCl pH 7.4, 150 mM NaCl, 10 mM MgCl$_2$, 0.05% Tween-20). HA concentration range in the assay mixture was 0.02–800 nM. All the samples were centrifuged at 14,000 ×g for 10 min to remove any aggregates present. The samples were loaded into Monolith NT.115 capillaries after incubation at room temperature for 5 min and MST measurements were performed at 22 °C by using nano-blue excitation with LED excitation power 20% and 80% for Dex-2 and 3 respectively, infrared laser (MST power) was set to medium. Data analyses were performed using Nanotemper analysis software. For determination of the dissociation constant (K_d) of the binding interaction, normalized fluorescence values were plotted against log of the estimated hyaluronic acid concentration in the porcine vitreous using GraphPad Prism software (version7.04, San Diego, CA, USA).

2.2.3. Binding of Dexamethasone-Arginine fragment to glucocorticoid receptor

Microscale thermophoresis (MST) technique was used to study the binding interaction of Dexamethasone-Arginine (Dex-Arg) fragment and glucocorticoid receptor. The MST measurements were performed using a Monolith NT.115 instrument from Nanotemper Technologies with MST grade premium NT.115 capillaries. Purified human glucocorticoid receptor (hGR, Abcam) was labeled with Lightning-Link® Rapid Alexa Fluor® 488 kit (Expedeon) following manufacturer's instruction. The labeling kit enables direct conjugation of Alexa Fluor® 488 with the available amine groups in the hGR. Unlabeled Dex-Arg fragment was serially diluted from 0.5 μM to 0.015 nM in MST optimized buffer and titrated into a fixed concentration of labeled hGR (10 nM). All the samples were centrifuged at 14,000 ×g for 10 min to remove aggregates. The samples were loaded into Monolith NT.115 premium capillaries after incubation at room temperature for 10 min and MST measurements were performed at 22 °C by using 5% LED power and medium MST power. Data analyses were done using Nanotemper analysis software. Normalized fluorescence values were plotted against the log of Dex-Arg fragment concentration using GraphPad Prism software (version7.04, San Diego, CA, USA).

2.2.4. Molecular docking to glucocorticoid receptor

For computational modeling of the Dex-Arg fragment, we utilized the crystal structure of human glucocorticoid receptor (hGR) in complex with dexamethasone (PDB id: 1M2Z). The protein-ligand complex exists as a dimer in the crystal structure. Only a single chain of the receptor was considered for molecular docking. Dexamethasone and other small molecules (including water) were removed from the ligand-

binding domain to generate the native structural model of the hGR as the target protein. 3D-structural models of dexamethasone and Dex-Arg fragment were built by using MarvinSketch (version 20.11.0; http://www.chemaxon.com). CB-Dock server [30] was used to predict the binding modes of dexamethasone and Dex-Arg fragment with the hGR. The best docking results were then compared with the crystal structure complex and visualized using UCSF Chimera package [31].

2.3. Cell culture and cell based assays

ARPE-19 cells (human retinal pigment epithelial cell line, ATCC CRL-2302) were cultured in Dulbecco's Modified Eagle Medium: Nutrient Mixture F-12 (DMEM/F-12) supplemented with 10% fetal bovine serum (Gibco), 100 U/ml penicillin, 100 μg/ml streptomycin and 2 mM L-glutamine (Gibco). The cells were cultured in a T-75 flask at 37 °C in a 7% CO_2 atmosphere. The cells were sub-cultured once a week until they reached 80% confluency. The culture media was changed twice a week.

2.3.1. Cytotoxicity

Cytotoxicity of the peptide-dexamethasone conjugates was evaluated using MTT assay as previously described [32]. Briefly, the cells were seeded in 96-well plates at a density of 20,000 cells per well in 150 μl of cell growth medium. After over-night incubation, the cells were washed with PBS. Peptides at various concentrations (0.01–100 μM) in complete cell growth medium (100 μl) were added to each well for incubation (5 h at 37 °C, 7% CO_2). Poly-L-lysine (PLL) treated and untreated cells served as negative and positive controls, respectively. After incubation, the medium was aspirated, the cells were washed with PBS and 150 μl of growth medium was added to the cells. Then, the cells were washed with PBS after incubation of 24 h. A mixture of 90 μl of complete growth medium and 10 μl of 5 mg/ml of MTT solution was added to the wells and the plates were incubated for 4 h at 37 °C. After incubation, 100 μl of 10% sodium dodecyl sulfate (Merck) in 0.01 M HCl (Sigma-Aldrich) was added to the wells to solubilize formazan crystals followed by overnight incubation at 37 °C. Formazan was quantified by measuring absorbance at 570 nm using a spectral scanning multimode plate reader (Varioskan Flash, Thermo Scientific). Viability of the treated cells was compared to the untreated control cells.

2.3.2. Cellular uptake

ARPE-19 cells were seeded on a 24-well Sensoplate polystyrene flat glass bottom black plates (Greiner bio-one) at a density of 25,000 cells/well and incubated at 37 °C with 7% CO_2 for 24 h. The cells were rinsed twice with 2 ml HBSS buffer (Gibco, supplemented with 10 mM Hepes, pH 7.4) and equilibrated in the same buffer for 30 min at 37 °C. The cells were then treated with labeled peptide-dexamethasone conjugates (5 μM) for 1 h at 37 °C. Afterwards cells were washed thrice with HBSS buffer to remove unbound and surface bound conjugates followed by plasma membrane staining with CellMask™ Deep Red (Invitrogen) for 30 min at room temperature in dark. The nuclei were stained with 1 μg/ml Hoechst 33342 for 10 min at room temperature in dark, washed with HBSS to remove excess stain and live cells were imaged immediately using Cytation 5 cell imaging multimode reader (BioTek). Images were taken using $40\times$ plan fluorite phase objective (1,320,518, Olympus) and processed with Gen5 Image Prime software, version 3.08. All images were obtained under identical conditions; the cell nucleus, the cytoskeleton and the conjugates were visualized in blue, deep red and green, respectively.

2.3.3. Intracellular drug release

Intracellular release of dexamethasone from the peptide-dexamethasone conjugates was studied using sub-confluent ARPE-19 cells that were cultured on 6 well plate. The cells were seeded at a density of 500,000 cells/well and experiments were performed 48 h after the cells

had achieved sub-confluent monolayer. The conjugates were dissolved in complete growth medium (DMEM/F-12; supplemented with 100 U/ml streptomycin/penicillin and 2 mM L-glutamine). Prior to the experiment, the cells were washed twice with PBS (Gibco) and incubated with the conjugates (5 μM/well) for 1 h at 37 °C. After 1 h, the cells were washed thrice with PBS to remove unbound and surface bound conjugates. The cells were detached from the bottom of the wells using TrypLE Express enzyme (Gibco) and the number of cells harvested from each well was determined. Lysis buffer (Biovision) was added to the cells collected from each well and the cells were lysed following the manufacturer's instructions. Clear cell lysate from each well was collected into low binding Eppendorf tubes and stored on ice before UPLC-MS analyses.

2.4. LC-MS analyses

To identify the molecule released from the conjugates in the cells (Section 2.3.3), three volumes of cold acetonitrile were added to the cell lysate samples, vortexed and stored at room temperature for 1 h. The samples were centrifuged for 10 min at 12,000 $\times g$ to remove precipitates. The supernatant was freeze-dried and stored at -20 °C for further UPLC-MS analysis.

UPLC-MS profiling analyses were carried out with Orbitrap-MS System (Q Exactive Focus, Thermo Fisher, Bremen, Germany) using reversed phase (RP) chromatography with positive mode ESI. The RP separation was performed on a Zorbax Eclipse XDB-C18 column (100 mm × 2.1 mm, 1.8 μm; Agilent Technologies). The flow rate was 0.4 ml/min, and gradient elution of 2–100% was used with water with 0.1% v/v of formic acid (eluent A) and methanol (eluent B). The injection volume was 10 μL and the sample tray was maintained at 4 °C. For data acquisition, the mass range was 300–1100 amu and 320–1200 amu with a resolution of 70,000. Data acquisition and analysis was conducted with Xcalibur and Freestyle software.

2.5. Intravitreal pharmacokinetics

Pigmented 2.5–3.0 kg female Dutch belted rabbits (Linköping, Sweden) were used in the study. The animals were housed under normal diet at a set temperature of 21 °C, humidity and 12/12 h light-dark cycle. All animal experiments were approved by the national Animal Experiment Board in Finland. Free dexamethasone was not included for *in vivo* PK studies to limit the number of animals used and due to limitations of non-invasive fluorophotometry that was employed in the present study.

2.5.1. Intravitreal injections

The animals were anesthetized with medetomidine (Domitor vet 1 mg/ml; Orion Pharma, Espoo, Finland; dose 0.5 mg/kg) and ketamine (Ketalar/Ketaminol vet 50 mg/ml; Pfizer Oy Animal Health, Espoo, Finland; dose 0.5 ml/kg). Pupils were dilated with tropicamide (Oftan Tropicamid 5 mg/ml, Santen Pharmaceutical Co., Ltd., Tampere, Finland) and eyes were locally anesthetized with oxybuprocaine (Oftan Obucain 4 mg/ml, Santen Pharmaceutical Co., Ltd., Tampere, Finland). Viscotears 2 mg/g (carbomer) was used for ocular surface moistening. The 31G disposable needle was inserted, about 4.5 mm out of limbus, through the sclera into the vitreous and 40 μl of the peptide solution with the concentration 125 μM (dose of 5 nmol per eye) was injected into the vitreous. After withdrawing the needle, the eyes were covered with antibiotic ointment in order to avoid infections (chloramphenicol; Oftan Chlora 10 mg/g). Two rabbits were injected with labeled Dex-1 conjugate and two others with labeled Dex2 conjugate in both eyes ($n = 4$ eyes/peptide). Dex-3 was not included in the pharmacokinetics study, as this particular conjugate had too low fluorescence intensity for Fluorotron assays. This could be due to internal quenching of the fluorescence signal as a consequence of the solution conformation of the peptide conjugate. Atipamezole (Antisedan vet 5 mg/ml; 0.2 ml/kg),

was used after anesthesia to wake the animals.

2.5.2. Fluorotron measurements

In vivo fluorophotometry measurements were performed with ocular fluorophotometer (Fluorotron Master, OcuMetrics, CA, USA). The animals were kept under light sedation (Domitor vet 1 mg/ml; 0.3 ml/kg) during the measurements. Baseline autofluorescence values were measured prior to the intravitreal injections. After the injections, the fluorescence levels in the vitreous and aqueous humor were measured daily for 3 days. Bepanthen Eye (sodium hyaluronate 0.15% and dexpanthenol 2%) was used for eye surface moisturizing during the measurements. The average fluorescence signal of vitreous was calculated by averaging in the axial region of eye starting 3 mm anteriorly from retina to the posterior edge of the lens. The distance of 3 mm from the retina decreases artifacts related to the tailing effect of retinal peak [33]. For aqueous humor values, the average of the signal in the middle of the compartment was used and calculated using the program of Flourotron. GraphPad Prism (version7.04, San Diego, CA, USA) was used for fitting concentration vs time curves and calculation of the pharmacokinetic parameters.

3. Results

3.1. Stability of the conjugates in the vitreous humor

To investigate the stability of the peptide-dexamethasone conjugates in the vitreal environment, the conjugates were incubated with porcine vitreous at 37 °C. All three conjugates were chemically stable in the vitreous humor. No significant quantities of free dexamethasone were detected during the assay period of 6 weeks (Fig. 1). These results ensure that the dexamethasone release takes place only after internalization within the RPE cells. Small quantity of unreacted dexamethasone (< 5%) as impurity was present in all the conjugates (Fig. 1).

3.2. Binding of the conjugates to the vitreous humor

Binding of peptide-dexamethasone conjugates to porcine vitreous was evaluated with microscale thermophoresis. Fig. 2 shows the thermophoresis signal from the binding interaction of Alexa 488 labeled conjugates (Dex-2 and Dex-3) and HA present in the vitreous humor. Normalized fluorescence values (Fnorm) plotted against log of HA concentration in porcine vitreous to obtain the binding affinity. The dissociation constants (K_d) for the binding of Dex-2 and Dex-3 conjugates to the vitreal HA were 13.5 nM and 64.3 nM, respectively. Dex-1 conjugate was not included in the study due to its adherence to the capillary walls.

3.3. Cellular uptake

Internalization of peptide-dexamethasone conjugates to cultured ARPE-19 cells was investigated. Fluorescence microscope images shows that the conjugates were internalized within the ARPE-19 cells without association at the cell surface (Fig. 3).

3.4. Cytotoxicity

Fig. 4 summarizes the results of the cytotoxicity assay. ARPE-19 cells tolerate the conjugates well at the concentration range of 0.01–5 μM without significant differences among the conjugates. The cytotoxicity of free dexamethasone was evaluated and no cell toxicity was seen (Supplementary material, Fig. S1).

3.5. Cellular release of dexamethasone from the conjugates

Dexamethasone did not release as pure drug from the conjugates. Instead, a fragment Dexamethasone-Arginine (r-NH-N=Dex: Dex-Arg), with one Arg residue from the PCL was detected linked to the drug. Full sequences of the peptide-dexamethasone conjugates, the fragments detected in the cell lysate and molecular masses of the detected fragments are shown in Table 1.

3.6. Binding affinity of Dexamethasone-Arginine fragment to glucocorticoid receptor

Binding of Dex-Arg fragment (0.01 nM to 0.5 μM) to a fixed concentration of labeled hGR (10 nM) was studied with thermophoresis (Fig. 5). The thermophoresis signal indicates binding of Dex-Arg to hGR in a dose dependent manner.

3.7. Molecular docking of Dexamethasone-Arginine fragment to glucocorticoid receptor

The application of CB-Dock and Chimera visualization elucidated the binding modes of dexamethasone and the Dex-Arg fragment. Top 5 cavity sizes were identified and Vina scores for binding were obtained for each of the cavities. The largest identified cavity (sized 690) for dexamethasone docking was the same as the LBD in the crystal structure of the hGR-dexamethasone complex. A structural comparison of the docked dexamethasone (best binding score) in the LBD with that over in the crystal structure resulted in a near perfect match as evidenced by the low *r.m.s.d.* value of 0.33 Å. This validated the docking methodology. The Dex-Arg fragment was similarly docked and the best binding orientation (score) in the LBD (cavity sized 690) was considered. Structural comparisons of the docked Dex-Arg fragment in the LBD with dexamethasone bound in the crystal structure complex showed a good-fit between the two ligands. A *r.m.s.d.* value of 1.34 Å
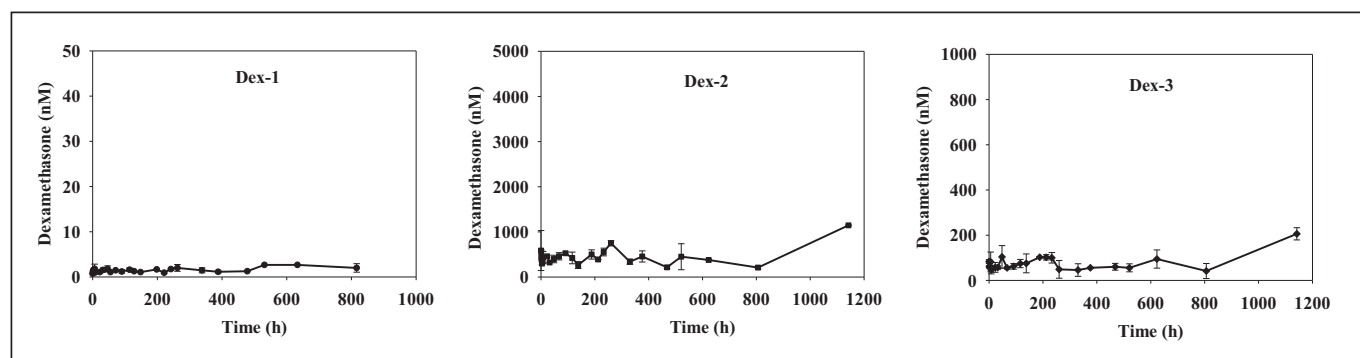

Fig. 1. Stability of peptide-dexamethasone conjugates in porcine vitreous. The conjugates were incubated with porcine vitreous and release of dexamethasone upon cleavage of the hydrazone bond in the conjugate was followed.
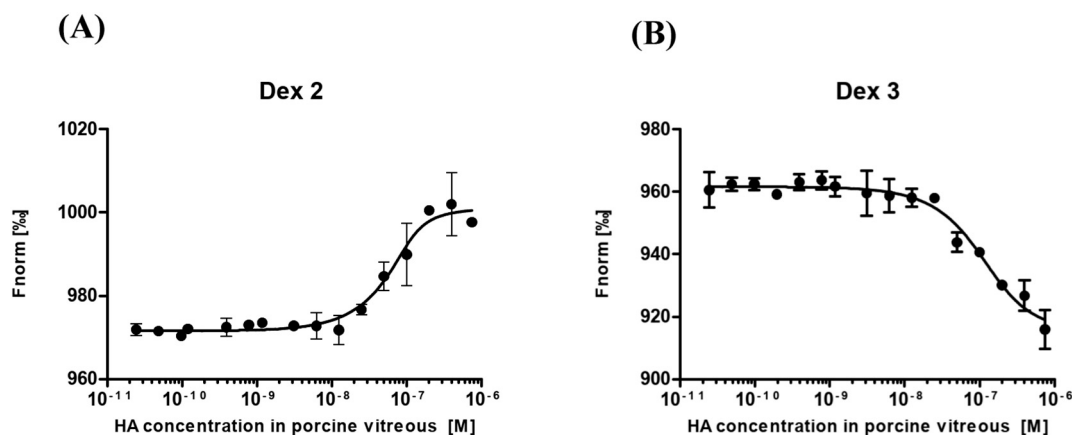
Fig. 2. Binding affinities of peptide-dexamethasone conjugates and porcine vitreous. Normalized fluorescence values (Fnorm) plotted against log of HA concentration in porcine vitreous to obtain the binding curves and the data fitted to obtain the K_d values. (A) Binding of fluorescently labeled Dex-2 with porcine vitreous, binding affinity (K_d) determined to be 13.5 nM (B) Binding of fluorescently labeled Dex-3 with porcine vitreous with a K_d value of 64.3 nM. Error bars represent standard error of $n = 3$ measurements.
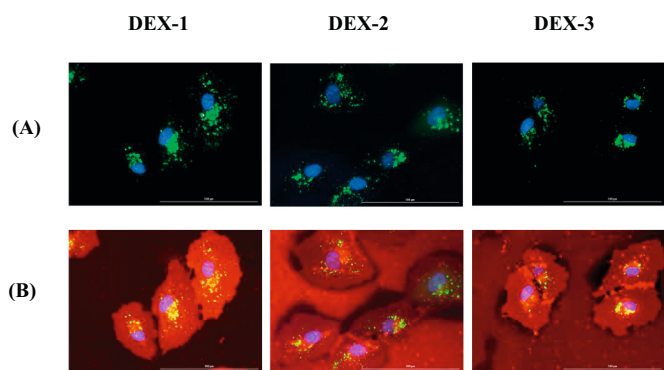
Fig. 3. Images of uptake of Alexa 488 labeled peptide-dexamethasone conjugates (5 μM) in living ARPE-19 cells, determined by Cytation 5 automated digital fluorescence imaging system. The peptides were incubated with the cells at 37 °C for 1 h. The cell nuclei and the conjugates (Alexa 488 labeled) were visualized with blue and green fluorescence respectively (A); cytoskeleton was visualized with deep red fluorescence (B). (For interpretation of the references to colour in this figure legend, the reader is referred to the web version of this article.)
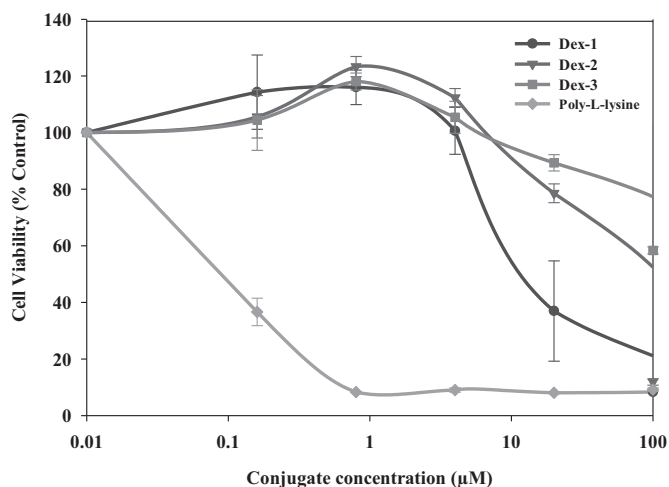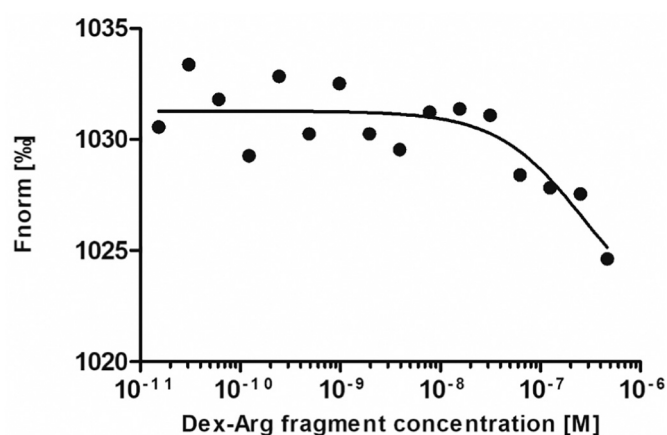

Fig. 5. Binding interaction of Dex-Arg fragment to human glucocorticoid receptor. Unlabeled Dex-Arg fragment (0.015 nM to 0.5 μM) was titrated into a fixed concentration of labeled hGR (10 nM). The thermophoretic signal (Fnorm) plotted as a function of log of Dex-Arg fragment concentration is shown.
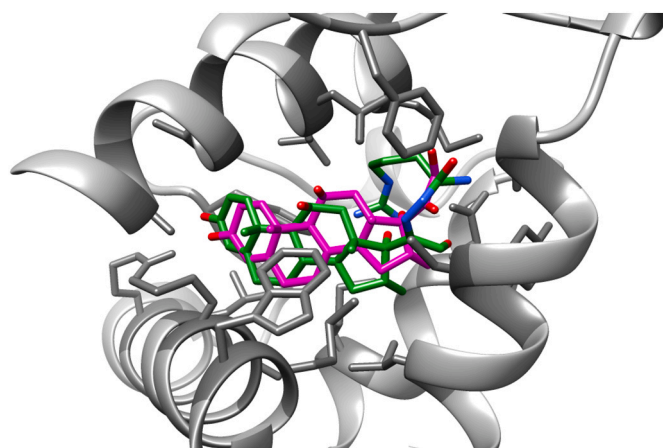

Fig. 4. Cytotoxicity of peptide-dexamethasone conjugates in ARPE-19 cells. Cells were treated with conjugates for 5 h and cell viability was evaluated with MTT cytotoxicity assay. The data were normalized based on the viability of untreated cells. Data are represented as mean ± standard deviation ($n = 3$).

Fig. 6. Structural comparison of the docked Dex-Arg fragment (green) with the structural model of dexamethasone (magenta) in complex with hGR (PDB id: 1M2Z). Residues of the ligand-binding domain have been depicted in dark grey. (For interpretation of the references to colour in this figure legend, the reader is referred to the web version of this article.)
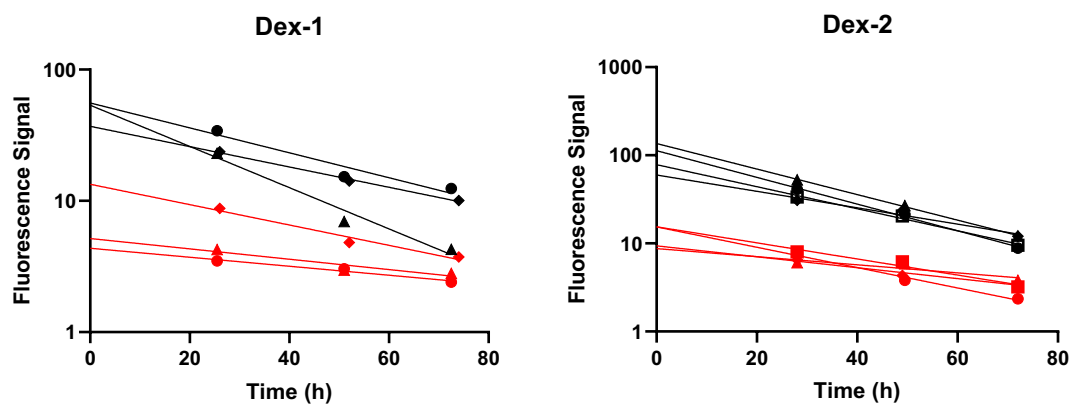
Fig. 7. Fluorophotometric signal versus time graphs of peptide-dexamethasone conjugates. Different symbols represent replicates from individual eyes. Black and red symbols correspond to signals from the vitreous and aqueous humor, respectively. (For interpretation of the references to colour in this figure legend, the reader is referred to the web version of this article.)

(matching the corresponding non-H atoms of the dexamethasone part of the molecule) was observed. Fig. 6 depicts the degree of structural superposition of the docked Dex-Arg fragment with that of the structural model of dexamethasone in complex with the hGR (PDB id: 1M2Z). The docking results validated that the Dex-Arg fragment binds at the same site as dexamethasone on the hGR.

3.8. In vivo pharmacokinetics

The results from the three rabbit eyes that received Dex-1 and four rabbit eyes that received Dex-2 (Scheme 1) injections intravitreally are shown in Fig. 7. The data from the fourth eye that was injected with Dex-1 is not included because some complications emerged after the injection. Vitreous and aqueous humor fluorescence signals of Dex-2 from a single rabbit eye (Supplementary Material, Fig. S2) shows a concentration gradient at 3 h after intravitreal injection. However, after 24 h, the conjugate was homogenously distributed in the vitreous (the first data point for PK calculations). The concentrations in the vitreous humor were approximately one order of magnitude higher than the concentrations in the aqueous humor. The vitreous and anterior chamber peptide conjugate concentrations were fitted with one-compartment model with first order elimination kinetics resulting in the elimination half-lives of 29.9 ± 10.0 h and 24.3 ± 5.6 h for Dex-1 and Dex-2, respectively. The anatomical vitreous volume was used as volume of drug distribution to calculate drug clearance (Table 2) (for most intravitreal compounds the volume of distribution (V_d) is in the range of anatomical vitreal volume [15]):

$$CL = V_d * K_v \qquad (1)$$

where CL is the vitreal clearance (μl/h), V_d is the anatomical volume of vitreous in rabbits (1700 μl) [34] and K_v is elimination constant (h^{-1}) from vitreous. The average clearance values of the peptide-

dexamethasone conjugates from the vitreous were approximately 40–50 μl/h.

To further ascertain the elimination route of the peptide-dexamethasone conjugates (anterior or posterior) after intravitreal injection, a method of Maurice and Mishima was used [35,36]. For anterior elimination pathway, the C_a/C_v ratio and vitreal elimination half-lives of the compounds can be expressed by the following equations:

$$\frac{Ca}{Cv} = \frac{Kv\ Vv}{f} \text{or} \frac{Ca}{Cv} = \frac{0.693\ Vv}{f\ t1/2} \qquad (2)$$

where C_a and C_v are the concentrations of the injected molecule in the anterior segment and the vitreous, respectively; K_v is elimination constant from vitreous; V_v is the average volume of vitreous compartment in rabbit (1700 μl) [34]; f is the aqueous humor flow rate (3 μl/min) [37] and $t_{1/2}$ is elimination half-life of the injected molecule from the vitreous. The calculated pharmacokinetic parameters of the peptide-dexamethasone conjugates (Dex-1, Dex-2) were in the close vicinity of the predicted blue trend line of the relationship in the Eq. (2) (Fig. 8). This suggests that the anterior route dominates in the vitreal elimination of the peptide conjugates. Fig. 8 also suggests that the elimination of Dex-1 and Dex-2 from the vitreous takes place as expected on the basis of their molecular weights. The elimination of the peptide conjugates via the anterior route is in contrast with that of free dexamethasone. Posterior clearance from the vitreous has been reported to be dominant for free dexamethasone [4]. The higher vitreal clearance rate of free dexamethasone (460 μl/h) as compared to the average flow-rate of aqueous humor (180 μl/h) also supports the major contribution of the posterior route of dexamethasone elimination.

4. Discussion

Intravitreal administration of small molecule drugs are associated

Table 2
Vitreal pharmacokinetic parameters of the conjugates after intravitreal injection.

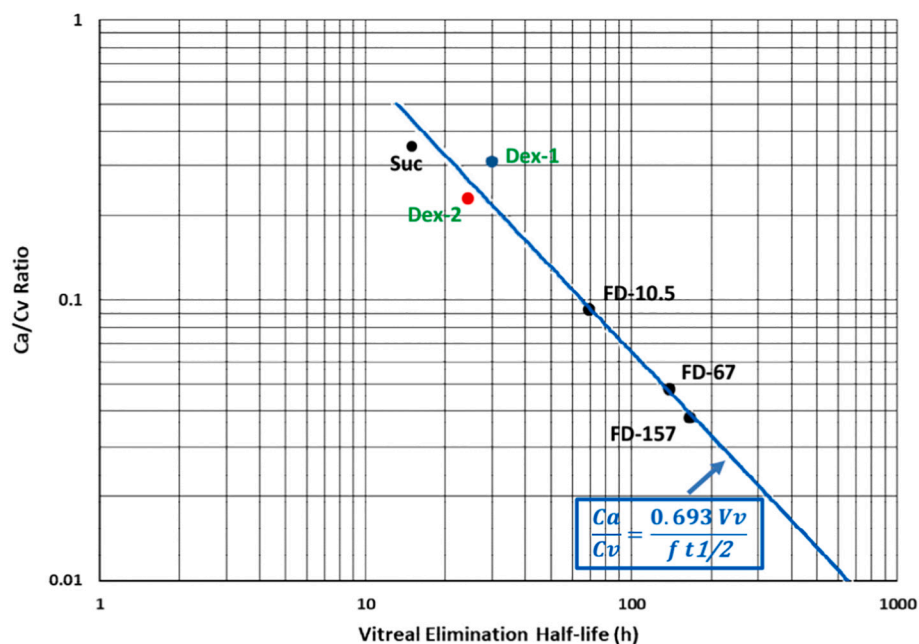|	Elimination half-life (h)	Elimination rate constant (h^{-1})	Vitreal clearance (μl/h)	C_a/C_v ratio
Dex-1				
Eye-1	31.7	0.021	35.7	0.16
Eye-2	19.2	0.036	61.2	0.42
Eye-3	38.90	0.017	28.9	0.36
Average ± SD	29.9 ± 10.0	0.024 ± 0.010	41.9 ± 17.0	0.31 ± 0.14
Dex-2				
Eye-1	19.9	0.034	57.8	0.20
Eye-2	20.8	0.033	56.1	0.21
Eye-3	32.3	0.021	35.7	0.22
Eye-4	24.1	0.028	47.6	0.29
Average ± SD	24.3 ± 5.7	0.029 ± 0.005	49.3 ± 10.1	0.23 ± 0.04

Fig. 8. Vitreal elimination half-life vs aqueous/vitreous concentration ratio of the peptide-dexamethasone conjugates following intravitreal injection in rabbit. Dex-1 and Dex-2 parameters falls in the vicinity of the blue trend line and are consistent with the other compounds with different molecular weight suggesting that the anterior pathway is the main route of their elimination. The data sources are as follows: sucrose (Suc) [38], FD-10.5, FD-67 and FD-157 [36]. The mean molecular weights of FITC-dextrans (FD) are 10.5 kD, 67 kD, respectively. The molecular weight of sucrose (Suc) is 0.342 kD. Dex-1 and Dex-2 has molecular weight of 4.43 and 4.29 kD, respectively. (For interpretation of the references to colour in this figure legend, the reader is referred to the web version of this article.)

with disadvantages, such as fast elimination rate, non-specific distribution to various ocular tissues and require frequent dosing [6,15]. Development of long acting and tissue specific drug delivery systems are needed to overcome such challenges. Polymer-drug conjugates (i.e. polymeric prodrugs) offer several potential advantages: increased solubility, prolonged drug retention, and targeted delivery of the therapeutics [39,40]. Although such approaches have been explored in the field of anticancer therapy [16,41]; their utility in the context of ocular drug delivery has been only sparsely investigated [18]. Conjugates are interesting option in intravitreal dug delivery, because they can be administered as clear solutions, and pharmacokinetics can be optimized in terms of cellular drug delivery and duration of action.

Dexamethasone is a corticosteroid that is used to treat inflammatory conditions in the anterior and posterior segments [19,42]. Intravitreal dexamethasone injections have been used to treat posterior segment inflammation, macular edema and neovascular macular degeneration [43] but short half-life of dexamethasone in the vitreous humor ($\approx$ 3 h) suggests that frequent intravitreal injections would be required to maintain levels of therapeutic concentration [44,45]. Therefore, dexamethasone has been delivered to the vitreous as biodegradable implants and coarse suspensions but these modes of drug delivery may interfere with vision and require larger needle or applicator for intravitreal placement. These approaches prolong duration of drug action without improvement in the drug distribution profiles. As such, typical adverse effects of corticosteroids (elevation of intraocular pressure, cataract formation) are unavoidable. In this study, we have explored a modular peptide-based delivery system for prolonged vitreal retention and drug delivery into the retinal pigment epithelial cells.

The modular delivery system is derived from our previous study [18] that demonstrated the release of short model peptides within the retinal pigment epithelial cells. The modular construct consists of the N-terminus segment for cellular delivery (cell penetrating peptide sequence) and a linker peptide that cleaves in intracellular environment. Dexamethasone was attached to the C-terminus of the linker peptide with hydrazone linkage (Scheme 1). Recent reports suggest that polycationic surface charge on particles bind electrostatically to the hyaluronic acid [27]. Li and co-workers reported the use of cationic nanoparticles, coated with L-Arg, as ocular drug delivery system with prolonged vitreal half-life [46]. In the design of our modular delivery system, we hypothesized to exploit this information. The N-terminus sequences were varied to contain differing amounts of positive charge

to serve dual purpose: intracellular localization and vitreal retention by interactions with the vitreal components. Binding to hyaluronic acid in the vitreous is expected to slow down the vitreal diffusion of the modular peptide conjugates resulting in increased retention time and low clearance. Indeed, the interaction studies of peptide-dexamethasone conjugates with porcine vitreous revealed that the Dex-2 conjugate with higher number of positive charges has higher binding affinity compared to Dex-3 conjugate (Fig. 2). The apparent K_d values are 13.5 nM and 64.3 nM for Dex-2 and Dex-3 conjugates, respectively.

Plots of vitreal elimination half-life and aqueous/vitreous concentration ratios for the peptide-dexamethasone conjugates [36] (Fig. 8) reveal that the anterior route is their main elimination pathway. Diffusion in the vitreous is a critically important parameter in the anterior elimination of intravitreal compounds [6]. Binding to the hyaluronic acid is expected to prolong intravitreal half-life. A recent study reported 3–4 fold increase in half-life of a protein when hyaluronic acid binding polypeptide sequence of 97 amino acids was fused to the structure [17]. In our study, the peptide-dexamethasone conjugates showed 8–10 fold increase in the vitreal half-life (24–30 h) as compared to the half-life of dexamethasone solution (3 h) [44,47]. This is due to the reduced elimination of dexamethasone across the blood ocular barriers. Fig. 8 demonstrates that the anterior elimination in the rabbit eyes was as expected based just on the molecular weight even though the peptides bind to hyaluronic acid. This may be explained by the binding equilibria. We used Coffey's approach [48,49] to simulate the impact of hyaluronic acid binding on vitreal drug elimination (for details, see Supplementary Material). After an injection of 5 nmol of peptide-dexamethasone conjugate into the vitreous, the initial concentration of the compound in the rabbit vitreous is about 3000 nM (approx. Volume 1.5 ml). Most of the conjugate is in free form after injection until $\approx$ 80% of the dose has been eliminated from the vitreous (Fig. 9A). The fraction of bound peptide increases at low concentrations (< 600 nM) (Fig. 9A) and half-life will increase significantly only at concentrations below 300 nM (Fig. 9B). These estimates were obtained based on binding profile (MST studies) data with the porcine vitreous. However, the impact of binding of hyaluronic acid on conjugate clearance is expected to be rather small in the rabbit vitreous as it has lower hyaluronic acid concentration than the pig vitreous [50,51]. Apparently, higher affinity and/or smaller doses are required for further prolongation of the vitreal retention.

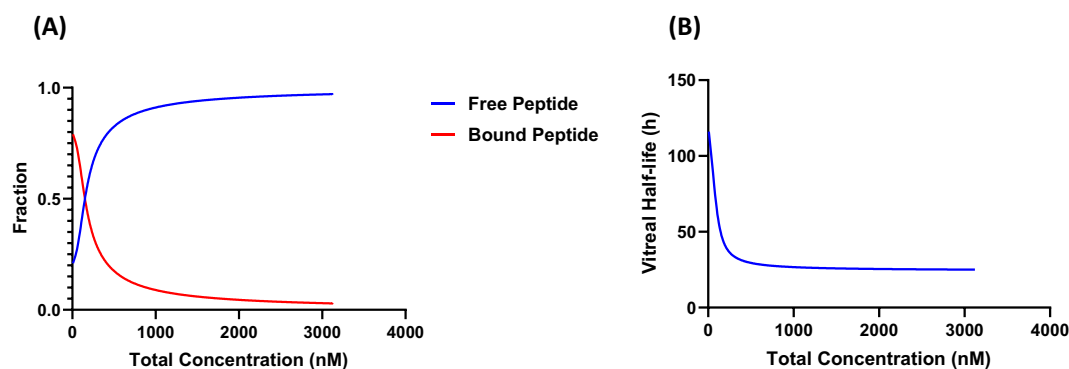Stability in the vitreous is one of the key requirements for the

Fig. 9. Fraction of bound and free Dex-2 peptide at different concentrations in the porcine vitreous (A). The correlation of vitreal elimination half-life of Dex-2 peptide and total concentration in the vitreous (B).

intravitreal applicability of modular drug delivery systems. Ex vivo stability data reveal that the dexamethasone-peptide conjugates were chemically stable for over 6 weeks in the porcine vitreous, suggesting that no significant enzymatic cleavage by the peptidases takes place in the vitreous humor. Thus, the peptide-dexamethasone conjugates stay intact until delivered to the intracellular environment in the retina. In a recent report, Matter et al. (2019) suggest that dexamethasone is not stable in water solutions [52]. It is noteworthy that only minimal concentrations of free dexamethasone (mostly residual amounts from conjugate synthesis) were seen in the vitreal incubation studies of 6 weeks. Consequently, degradation product levels, if any, is expected to be negligible. Furthermore, the available time for any degradation is only a few days based on *in vivo* kinetics (Fig. 7).

We postulate that the modular delivery system has potential therapeutic benefits, because the drug is released within the cells. Therefore, this may enable effect at lower dose and reduced drug distribution to the off-target cells, which may reduce adverse effects of the corticosteroid. This principle may be applicable also to other drugs. Furthermore, cellular internalization and drug release in the retinal pigment epithelial cells might turn these cells as reservoirs for drug release to the neighboring cells [18]. Many diseases of the posterior segment of the eye, such as age-related macular degeneration and proliferative vitreoretinopathy, have a common therapeutic target cell, the retinal pigment epithelium [53–55]. To this effect, the modular peptide-based delivery system meets the key objective of being able to release dexamethasone within the retinal pigment epithelial cells. Larger sized protein molecules, such as, the ciliary derived neurotropic factor (CNTF; mol wt. 23 kDa) is known to permeate into the retina [56]. We therefore postulate that the smaller sized peptide conjugates (mol wt. 4.5 kDa) will easily permeate across the inner limiting membrane to the retina. The peptide-dexamethasone conjugates demonstrated significant cellular uptake, aided by the N-terminal cell penetrating peptide (Fig. 3) and dexamethasone release by cathepsin D mediated enzymatic cleavage of the peptide linker. The released fragment Dex-Arg is in accordance with results from our previous study on sequence-activity relationship of the peptide based linkers [18]. The fragment Dex-Arg binds to the glucocorticoid receptor as evidenced by computational and experimental approaches.

The focus and scope of the present work was to highlight and demonstrate the utility of our modular peptide-based drug delivery system for application in ocular diseases. Although the fluorescence based technique, Fluorotron, does not monitor the levels of dexamethasone or Dex-Arg fragment in the vitreous or retina *in vivo*; data suggests that Dex-Arg fragment is generated in the retina (RPE cells). Chemical quantitation of all relevant molecular species will be a topic of future studies with promising conjugate(s).

Importantly, modular peptide conjugates are rather small molecules. This is important for retinal permeation across the inner limiting membrane [6] to the retinal layers. Secondly, these are soluble

molecules, allowing injection of transparent solutions. Thirdly, the conjugates are based on endogenous components (i.e. amino acids) which reduces the risk of toxicity. In addition, manufacturing of injectable solutions is less complex than production of particle based delivery systems.

5. Conclusions

We have shown the potential utility of a modular peptide-based delivery system for the retinal delivery of dexamethasone. The system is stable in the vitreous, internalizes within the retinal pigment epithelial cells and releases the drug after enzymatic cleavage of the peptide based linker. The modular peptide systems are promising candidates for ocular drug delivery and should be further optimized.

Declaration of competing interest

The authors declare no conflict of interest.

Appendix A. Supplementary data

Supplementary data to this article can be found online at https://doi.org/10.1016/j.jconrel.2020.09.005.

References

[1] A. Urtti, Challenges and obstacles of ocular pharmacokinetics and drug delivery, Adv. Drug Deliv. Rev. 58 (2006) 1131–1135, https://doi.org/10.1016/j.addr.2006.07.027.

[2] Barriers for posterior segment ocular drug delivery, in: R.J. Gaudana, M. Barot, A. Patel, V. Khurana, A.K. Mitra (Eds.), Treatise Ocul. Drug Deliv. BENTHAM SCIENCE PUBLISHERS, 2013, pp. 68–95, , https://doi.org/10.2174/9781608051755113010007.

[3] V. Gote, S. Sikder, J. Sicotte, D. Pal, Ocular drug delivery: present innovations and future challenges, J. Pharmacol. Exp. Ther. 370 (2019) 602–624, https://doi.org/10.1124/jpet.119.256933.

[4] D.M. Maurice, S. Mishima, Ocular Pharmacokinetics, Springer, Berlin, Heidelberg, 1984, pp. 19–116, https://doi.org/10.1007/978-3-642-69222-2_2.

[5] A. Urtti, J.D. Pipkin, G. Rork, A.J. Repta, Controlled drug delivery devices for experimental ocular studies with timolol 1. In vitro release studies, Int. J. Pharm. 61 (1990) 235–240, https://doi.org/10.1016/0378-5173(90)90214-O.

[6] E.M. del Amo, A.K. Rimpelä, E. Heikkinen, O.K. Kari, E. Ramsay, T. Lajunen, M. Schmitt, L. Pelkonen, M. Bhattacharya, D. Richardson, A. Subrizi, T. Turunen, M. Reinisalo, J. Itkonen, E. Toropainen, M. Casteleijn, H. Kidron, M. Antopolsky, K.S. Vellonen, M. Ruponen, A. Urtti, Pharmacokinetic aspects of retinal drug delivery, Prog. Retin. Eye Res. 57 (2017) 134–185, https://doi.org/10.1016/j.preteyeres.2016.12.001.

[7] K.S. Vellonen, E.M. Soini, E.M. Del Amo, A. Urtti, Prediction of ocular drug distribution from systemic blood circulation, Mol. Pharm. 13 (2016) 2906–2911, https://doi.org/10.1021/acs.molpharmaceut.5b00729.

[8] H.F. Edelhauser, C.L. Rowe-Rendleman, M.R. Robinson, D.G. Dawson, G.J. Chader, H.E. Grossniklaus, K.D. Rittenhouse, C.G. Wilson, D.A. Weber, B.D. Kuppermann, K.G. Csaky, T.W. Olsen, U.B. Kompella, V.M. Holers, G.S. Hageman, B.C. Gilger, P.A. Campochiaro, S.M. Whitcup, W.T. Wong, Ophthalmic drug delivery systems for the treatment of retinal diseases: basic research to clinical applications, Investig. Ophthalmol. Vis. Sci. 51 (2010) 5403–5420, https://doi.org/10.1167/iovs.10-5392.

[9] N. Kuno, S. Fujii, Recent advances in ocular drug delivery systems, Polymers (Basel) 3 (2011) 193–221.

[10] E. Delamo, A. Urtti, Current and future ophthalmic drug delivery systems: a shift to the posterior segment, Drug Discov. Today 13 (2008) 135–143.

[11] R. Nagaraj, D.R. Bijukumar, B. Mathew, E.A. Scott, M.T. Mathew, A review on recent advancements in ophthalmology devices: currently in market and under clinical trials, J. Drug Deliv. Sci. Technol. 52 (2019) 334–345, https://doi.org/10.1016/j.jddst.2019.04.038.

[12] F. Pacella, A.F. Ferraresi, P. Turchetti, T. Lenzi, R. Giustolisi, A. Bottone, V. Fameli, M.R. Romano, E. Pacella, Intravitreal injection of Ozurdex® implant in patients with persistent diabetic macular edema, with six-month follow-up, Ophthalmol. Eye Dis. 8 (2016) OED.S38028, https://doi.org/10.4137/oed.s38028.

[13] T.V. Chirila, D.G. Harkin, Biomaterials and Regenerative Medicine in Ophthalmology: Second Edition, Elsevier Inc, 2016, https://doi.org/10.1016/C2014-0-01443-8.

[14] K. Nayak, M. Misra, A review on recent drug delivery systems for posterior segment of eye, Biomed. Pharmacother. 107 (2018) 1564–1582, https://doi.org/10.1016/j.biopha.2018.08.138.

[15] E.M. Del Amo, K.S. Vellonen, H. Kidron, A. Urtti, Intravitreal clearance and volume of distribution of compounds in rabbits: in silico prediction and pharmacokinetic simulations for drug development, Eur. J. Pharm. Biopharm. 95 (2015) 215–226, https://doi.org/10.1016/j.ejpb.2015.01.003.

[16] J.H. Park, S. Lee, J.H. Kim, K. Park, K. Kim, I.C. Kwon, Polymeric nanomedicine for cancer therapy, Prog. Polym. Sci. (2008), https://doi.org/10.1016/j.progpolymsci.2007.09.003.

[17] J.G. Ghosh, A.A. Nguyen, C.E. Bigelow, S. Poor, Y. Qiu, N. Rangaswamy, R. Ornberg, B. Jackson, H. Mak, T. Ezell, V. Kenanova, E. De La Cruz, A. Carrion, B. Etemad-Gilbertson, R.G. Caro, K. Zhu, V. George, J. Bai, R. Sharma-Nahar, S. Shen, Y. Wang, K.K. Subramanian, E. Fassbender, M. Maker, S. Hanks, J. Vrouvlianis, B. Leehy, D. Long, M. Prentiss, V. Kansara, B. Jaffee, T.P. Dryja, M. Roguska, Long-acting protein drugs for the treatment of ocular diseases, Nat. Commun. 8 (2017) 1–10, https://doi.org/10.1038/ncomms14837.

[18] M. Bhattacharya, S. Sarkhel, J. Peltoniemi, R. Broadbridge, M. Tuomainen, S. Auriola, A. Urtti, Differentially cleaving peptides as a strategy for controlled drug release in human retinal pigment epithelial cells, J. Control. Release 251 (2017) 37–48.

[19] J. Rodríguez Villanueva, L. Rodríguez Villanueva, M. Guzmán Navarro, Pharmaceutical technology can turn a traditional drug, dexamethasone into a first-line ocular medicine. A global perspective and future trends, Int. J. Pharm. 516 (2017) 342–351, https://doi.org/10.1016/j.ijpharm.2016.11.053.

[20] B. Abadia, P. Calvo, A. Ferreras, F. Bartol, G. Verdes, L. Pablo, Clinical applications of dexamethasone for aged eyes, Drugs Aging 33 (2016) 639–646, https://doi.org/10.1007/s40266-016-0392-z.

[21] F. Milletti, Cell-penetrating peptides: classes, origin, and current landscape, Drug Discov. Today 17 (2012) 850–860, https://doi.org/10.1016/j.drudis.2012.03.002.

[22] E. Atherton, R.C. Sheppard, Solid Phase Peptide Synthesis: A Practical Approach, IRL Press at Oxford University Press, 1989.

[23] M. Jerabek-Willemsen, T. André, R. Wanner, H.M. Roth, S. Duhr, P. Baaske, D. Breitsprecher, MicroScale thermophoresis: interaction analysis and beyond, J. Mol. Struct. 1077 (2014) 101–113, https://doi.org/10.1016/j.molstruc.2014.03.009.

[24] C.J. Wienken, P. Baaske, U. Rothbauer, D. Braun, S. Duhr, Protein-binding assays in biological liquids using microscale thermophoresis, Nat. Commun. 1 (2010) 1–7, https://doi.org/10.1038/ncomms1093.

[25] S.A.I. Seidel, P.M. Dijkman, W.A. Lea, G. van den Bogaart, M. Jerabek-Willemsen, A. Lazic, J.S. Joseph, P. Srinivasan, P. Baaske, A. Simeonov, I. Katritch, F.A. Melo, J.E. Ladbury, G. Schreiber, A. Watts, D. Braun, S. Duhr, Microscale thermophoresis quantifies biomolecular interactions under previously challenging conditions, Methods 59 (2013) 301–315, https://doi.org/10.1016/j.ymeth.2012.12.005.

[26] H. Kim, S.B. Robinson, K.G. Csaky, Investigating the movement of intravitreal human serum albumin nanoparticles in the vitreous and retina, Pharm. Res. 26 (2009) 329–337, https://doi.org/10.1007/s11095-008-9745-6.

[27] I. Melgar-Asensio, I. Kandela, F. Aird, S.R. Darjatmoko, C. de los Rios, C.M. Sorenson, D.M. Albert, N. Sheibani, J. Henkin, Extended intravitreal rabbit eye residence of nanoparticles conjugated with cationic arginine peptides for intraocular drug delivery: in vivo imaging, Investig. Ophthalmol. Vis. Sci. 59 (2018) 4071–4081, https://doi.org/10.1167/iovs.18-24087.

[28] A.V. Noulas, A.D. Theocharis, E. Feretis, N. Papageorgakopoulou, N.K. Karamanos, D.A. Theocharis, Pig vitreous gel: macromolecular composition with particular reference to hyaluronan-binding proteoglycans, Biochimie 84 (2002) 295–302, https://doi.org/10.1016/S0300-9084(02)01389-5.

[29] S. Shafaie, V. Hutter, M.B. Brown, M.T. Cook, D.Y.S. Chau, Diffusion through the ex vivo vitreal body – bovine, porcine, and ovine models are poor surrogates for the human vitreous, Int. J. Pharm. 550 (2018) 207–215, https://doi.org/10.1016/j.ijpharm.2018.07.070.

[30] Y. Liu, M. Grimm, W. tao Dai, M. chun Hou, Z.X. Xiao, Y. Cao, CB-Dock: a web server for cavity detection-guided protein–ligand blind docking, Acta Pharmacol. Sin. 41 (2020) 138–144, https://doi.org/10.1038/s41401-019-0228-6.

[31] E.F. Pettersen, T.D. Goddard, C.C. Huang, G.S. Couch, D.M. Greenblatt, E.C. Meng, T.E. Ferrin, UCSF Chimera – a visualization system for exploratory research and analysis, J. Comput. Chem. 25 (2004) 1605–1612.

[32] T. Mosmann, Rapid colorimetric assay for cellular growth and survival: application to proliferation and cytotoxicity assays, J. Immunol. Methods 65 (1983) 55–63, https://doi.org/10.1016/0022-1759(83)90303-4.

[33] F. Kayazawa, K. Miyake, Ocular fluorophotometry in patients with essential hypertension, Arch. Ophthalmol. 102 (1984) 1169–1170, https://doi.org/10.1001/archopht.1984.01040030947020.

[34] P.J. Missel, Simulating intravitreal injections in anatomically accurate models for rabbit, monkey, and human eyes, Pharm. Res. 29 (2012) 3251–3272.

[35] D.M. Maurice, S. Mishima, Ocular pharmacology, in: M. Sears (Ed.), Handb. Exp. Pharmacol, Springer-Verlag, Berlin-Heidelberg, 1984, pp. 16–119.

[36] F. Johnson, D. Maurice, A simple method of measuring aqueous humor flow with intravitreal fluoresceinated dextrans, Exp. Eye Res. 39 (1984) 791–805.

[37] C.B. Toris, Aqueous humor dynamics I: measurement methods and animal studies, Curr. Top. Membr. 62 (2008) 193–229.

[38] L.Z. Bito, E.V. Salvador, Intraocular fluid dynamics. III. The site and mechanism of prostaglandin transfer across the blood intraocular fluid barriers, Exp. Eye Res. 14 (1972) 233–241.

[39] I. Ekladious, Y.L. Colson, M.W. Grinstaff, Polymer–drug conjugate therapeutics: advances, insights and prospects, Nat. Rev. Drug Discov. 18 (2019) 273–294, https://doi.org/10.1038/s41573-018-0005-0.

[40] N. Larson, H. Ghandehari, Polymeric conjugates for drug delivery, Chem. Mater. 24 (2012) 840–853, https://doi.org/10.1021/cm2031569.

[41] Q. Feng, R. Tong, Anticancer nanoparticulate polymer-drug conjugate, Bioeng. Transl. Med. 1 (2016) 277–296, https://doi.org/10.1002/btm2.10033.

[42] R.S. Hunter, A.M. Lobo, Dexamethasone intravitreal implantfor the treatment of noninfectious uveitis, Clin. Ophthalmol. 5 (2011) 1612–1621, https://doi.org/10.2147/opth.s17419.

[43] B.D. Kuppermann, M. Goldstein, R.K. Maturi, A. Pollack, M. Singer, A. Tufail, D. Weinberger, X.-Y. Li, C.-C. Liu, J. Lou, S.M. Whitcup, Dexamethasone intravitreal implant as adjunctive therapy to ranibizumab in neovascular age-related macular degeneration: a multicenter randomized controlled trial, Ophthalmologica 234 (2015) 40–54, https://doi.org/10.1159/000381865.

[44] H.W. Kwak, D.J. D'Amico, Evaluation of the retinal toxicity and pharmacokinetics of dexamethasone after Intravitreal injection, Arch. Ophthalmol. 110 (1992) 259, https://doi.org/10.1001/archopht.1992.01080140115038.

[45] R. Bhagat, J. Zhang, S. Farooq, X.Y. Li, Comparison of the release profile and pharmacokinetics of intact and fragmented dexamethasone intravitreal implants in rabbit eyes, J. Ocul. Pharmacol. Ther. 30 (2014) 854–858, https://doi.org/10.1089/jop.2014.0082.

[46] H. Li, W. Liu, C.M. Sorenson, N. Sheibani, D.M. Albert, T. Senanayake, S. Vinogradov, J. Henkin, H.F. Zhang, Sustaining intravitreal residence with L-arginine peptide-conjugated nanocarriers, Investig. Ophthalmol. Vis. Sci. 58 (2017) 5142–5150, https://doi.org/10.1167/iovs.17-22160.

[47] K. Papangkorn, J.W. Higuchi, J. Brar, W.I. Higuchi, Ocular drug distribution and safety of a noninvasive ocular drug delivery system of dexamethasone sodium phosphate in rabbit, J. Ocul. Pharmacol. Ther. 34 (2018) 325–334, https://doi.org/10.1089/jop.2017.0093.

[48] J.J. Coffey, F.J. Bullock, P.T. Schoenemann, Numerical solution of nonlinear pharmacokinetic equations: effects of plasma protein binding on drug distribution and elimination, J. Pharm. Sci. 60 (1971) 1623–1628, https://doi.org/10.1002/jps.2600601106.

[49] J.J. Coffey, Effects of protein binding of drugs on areas under plasma concentration—time curves, J. Pharm. Sci. 61 (1972) 138–139, https://doi.org/10.1002/jps.2600610134.

[50] S.A. Boruchoff, A.M. Woodin, Viscosity and composition of solutions derived from rabbit vitreous humour, Br. J. Ophthalmol. 40 (1956) 113–118, https://doi.org/10.1136/bjo.40.2.113.

[51] E.A. Balazs, Functional anatomy of the vitreous, Duane's found, Clin. Ophthalmol. 1 (1993) 1–16.

[52] B. Matter, A. Ghaffari, D. Bourne, Y. Wang, S. Choi, U.B. Kompella, Dexamethasone degradation in aqueous medium and implications for correction of in vitro release from sustained release delivery systems, AAPS PharmSciTech 20 (2019) 1–11, https://doi.org/10.1208/s12249-019-1508-7.

[53] C. Larcher, H. Recheis, R. Sgonc, W. Göttinger, H.P. Huemer, E.U. Irschick, Influence of viral infection on expression of cell surface antigens in human retinal pigment epithelial cells, Graefes Arch. Clin. Exp. Ophthalmol. 235 (1997) 709–716.

[54] A.C. Bird, Therapeutic targets in age-related macular disease, J. Clin. Invest. 120

(2010) 3033–3041.

[55] I. Bhutto, G. Lutty, Understanding age-related macular degeneration (AMD): re-
lationships between the photoreceptor/retinal pigment epithelium/Bruch's mem-
brane/choriocapillaris complex, Mol. Asp. Med. 33 (2012) 295–317.

[56] J. Itkonen, A. Annala, S. Tavakoli, B. Arango-Gonzalez, M. Ueffing, E. Toropainen, M. Ruponen, M.G. Casteleijn, A. Urtti, Characterization, stability, and in vivo effi-
cacy studies of recombinant human CNTF and its permeation into the neural retina
in ex vivo organotypic retinal explant culture models, Pharmaceutics 12 (2020)
1–31, https://doi.org/10.3390/pharmaceutics12070611.